Jurnal Ilmu Fisika
Vol. 19, No. 1, March 2027, pp. 1–10
ISSN: 1979-4657 (Print); 2614-7386 (Online)
https://doi.org/10.25077/jif.19.1.1-10.2027

Jurnal Ilmu Fisika
Open Access

Effects of Layer Repetition and Cu Spacer Thickness on the Magnetoimpedance of Electrodeposited Permalloy Multilayers at 100 kHz and Its Application as a Magnetic Nanoparticle Sensor

Artono Dwijo Sutomo[1*], Febriani Wulandaria[1], Pratiwi Kusumawardhani[1], Riyatun Riyatun[1], Nurdiyantoro Putra Prasetya[2], Ismail Ismail[3], Budi Purnama[1]

[1]Physics Department, Faculty of Mathematics and Natural Sciences, Universitas Sebelas Maret, Surakarta 57126, Indonesia
[2]Physics Department, Faculty of Mathematics and Natural Sciences, Universitas Tanjungpura, Pontianak 78124, Indonesia
[3] Indonesian Polytechnic of Nuclear Technology, National Research and Innovation Agency, Yogyakarta 55281, Indonesia

Article Info

Article History:

Received June 24, 2026
Revised September 29, 2026
Accepted September 30, 2026
Published online October 28, 2026

Keywords:

magnetoimpedance
NiFe/Cu multilayers
electrodeposition
magnetic nanoparticles
magnetic sensing

Corresponding Author:

Artono Dwijo Sutomo
Email: artono@staff.uns.ac.id

ABSTRACT

Optimizing multilayer structures is essential for improving magnetoimpedance (MI) responses in low-frequency magnetic sensing applications. This study investigates the effects of layer repetition number (N) and Cu spacer thickness (x) on the magnetoimpedance (MI) response of [NiFe(600 nm)/Cu(x)/NiFe(600 nm)]N/Cu(200 nm)/[NiFe(600 nm)/Cu(x)/NiFe(600 nm)]N multilayer structures electrodeposited onto Cu printed circuit board substrates with meander patterns. The MI response was systematically evaluated at an operating frequency of 100 kHz to determine the optimal multilayer configuration. The results reveal that both layer repetition and Cu spacer thickness significantly influence the MI ratio. The highest MI ratio of 2.07% was achieved at N = 3 and x = 100 nm, suggesting an optimal balance between magnetic permeability and electrical conductivity. The sensing capability of the optimized multilayer structure was further evaluated using cobalt ferrite nanoparticles. Changes in the MI ratio of 0.32 and 0.64 were observed for nanoparticle masses of 0.1 and 0.3 g, respectively, indicating a mass-dependent sensor response. These findings demonstrate the potential of electrodeposited NiFe/Cu multilayer structures as low-frequency magnetoimpedance sensing platforms for magnetic nanoparticle detection.

Copyright © 2026 Author(s)

1. INTRODUCTION

The magnetoimpedance (MI) effect, characterized by the dependence of the electrical impedance of a magnetic conductor on an externally applied magnetic field, has attracted considerable attention due to its potential for developing highly sensitive magnetic sensors. Early observations of magnetic-field-dependent alternating-current impedance in high-permeability wires were reported in early scientific investigations. Decades later, this principle enabled the development of early magnetic field sensors utilizing amorphous ribbons. The modern era of magnetoimpedance (MI) research emerged with the rediscovery of high MI responses in amorphous wire systems (Beach & Berkowitz, 1994; Panina & Mohri, 1994). Building upon these foundational mechanisms, attention shifted toward planar geometry and nanostructuring. In 2004, the concept of magnetic nanostructuring in permalloy films was introduced and subsequently advanced across various thin-film system architectures, such as FeNi/Ag, to optimize field sensitivity and domain structures (Kurlyandskaya et al., 2004). Recent research further

Attribution-NonCommercial 4.0 International

examines the role of magnetic anisotropy and interlayer coupling in permalloy-based MI structures (Chlenova et al., 2017; Kilic et al., 2018).

Among the various MI configurations, magnetic multilayers consisting of ferromagnetic and nonmagnetic metallic layers have attracted increasing interest because their electrical and magnetic properties can be controlled through layer thickness, interlayer coupling, and structural arrangement. In particular, NiFe-based multilayers offer favorable soft-magnetic characteristics, while Cu interlayers provide conductive pathways and influence magnetic interactions between adjacent ferromagnetic layers. The incorporation of meander-patterned geometries further provides opportunities to increase the effective sensing length within a compact device and modify its magnetic response (Sutomo et al., 2023). Compared to single-layer structures, multilayer and meander architectures yield significantly higher MI responses at high operating frequencies (Licarião et al., 2025). Proper optimization of deposition parameters, geometry, layer thickness, and interlayer coupling can yield exceptionally high MI ratios exceeding 100% and sensitivities reaching up to 300%/Oe (García-Arribas et al., 2016). These results highlight the importance of structural optimization in improving MI performance. Theoretical and geometric studies show that multilayer symmetry and meander layout can modify current distribution and field-dependent impedance (Buznikov & Kurlyandskaya, 2019; de Melo et al., 2020; Kikuchi et al., 2020). Measurements of electrodeposited NiFe/Cu and meander sensing elements demonstrate that structural arrangements and operating conditions affect the MI response (Oktaria et al., 2020; Rusydan et al., 2021; Sayad et al., 2021). Electrodeposition conditions and associated mechanical stress can also alter the magnetic and electrical response of NiFe/Cu elements (Vasam & Veeturi, 2022; Tandon et al., 2023).

Beyond magnetic-field detection, MI-based sensors have demonstrated considerable potential for detecting magnetic nanoparticles (MNPs), which are widely investigated as magnetic labels and functional materials in biomedical and sensing applications. The feasibility of MI-based nanoparticle detection was demonstrated in earlier research on magnetic nanoparticle sensing. Since these initial demonstrations, MI biosensing has evolved through various structural formats, encompassing both wire-based platforms and microfluidic integration for ferrofluid detection (Barrera et al., 2024), as well as structured thin-film meander elements developed for investigating the response to magnetic particles. To interpret the underlying sensing mechanism, theoretical models have been developed to simulate the impedance response in the presence of magnetic media, such as ferrogels or tissue-embedded nanoparticles, by assessing local magnetic flux perturbations and changes in effective permeability (Buznikov et al., 2018). These developments demonstrate the versatility of MI-based sensing platforms and emphasize the importance of optimizing sensor structures to obtain measurable responses to magnetic nanoparticles. Recent particle-detection investigations and reviews demonstrate the importance of stray fields, measurement geometry, and sensor calibration when assessing the performance of MI sensing elements (Beato-López et al., 2021; Melnikov et al., 2021; Jimenez et al., 2022).

Despite these advances, optimizing the magnetoimpedance (MI) response at relatively low operating frequencies remains a challenge for practical sensing applications. The MI response is influenced by magnetic permeability, electrical conductivity, current distribution, and magnetic interactions, which can be modified by the number of magnetic layers and the thickness of nonmagnetic spacers. Although previous studies have demonstrated enhanced MI performance using multilayer and meander configurations, the combined effects of layer repetition number and Cu spacer thickness on symmetric NiFe/Cu multilayers fabricated on Cu printed circuit board (PCB) meander substrates remain insufficiently explored, particularly at low frequencies. Furthermore, the relationship between multilayer optimization and magnetic nanoparticle detection requires investigation (Beato-López et al., 2018). Cobalt ferrite nanoparticles provide a suitable model material for evaluating sensor performance because their magnetic properties can modify the local magnetic environment and, consequently, the MI response (Barrera et al., 2024). A systematic evaluation of these structural parameters and their influence on nanoparticle-induced MI changes could provide valuable insights into the relationship between multilayer design and sensing performance. Therefore, investigating both structural optimization and nanoparticle-induced impedance changes is essential for assessing the potential of electrodeposited

NiFe/Cu multilayers as low-frequency magnetic sensing platforms. Relevant studies on symmetry-dependent multilayer MI and magnetostatic interactions provide a basis for evaluating the combined effects of repetition number and Cu spacer thickness (Rusydan et al., 2022; Melnikov et al., 2024).

This study examines the influence of multilayered configuration parameters, namely the number of layer repetitions (N) and the Cu spacer-layer thickness (x), on the magnetoimpedance (MI) ratio of a symmetric permalloy multilayer system with the architecture of [NiFe(600 nm)/Cu(x)/NiFe(600 nm)]$_N$/Cu (200 nm)/[NiFe(600 nm)/Cu(x)/NiFe(600 nm)]$_N$. The structural and deposition parameters are analyzed to evaluate the resulting MI response in the low-frequency regime (~kHz order), and the optimized configuration is subsequently evaluated for magnetic nanoparticle sensing proof of concept. The main contribution of this study is the combined evaluation of multilayer structural parameters and preliminary magnetic nanoparticle sensing performance within a low-frequency MI platform, providing insights into the design of electrodeposited NiFe/Cu multilayer sensing elements.

2. METHOD

The multilayer samples of [NiFe(600 nm)/Cu(x)/NiFe(600 nm)]$_N$/Cu (200 nm)/[NiFe(600 nm)/Cu(x)/NiFe(600 nm)]$_N$ in this study were prepared using the electrodeposition method. Electrodeposition was carried out at room temperature with a Pt electrode. A meander-patterned Cu PCB substrate was employed for the experiment (meander width of 250 micrometers with a total path length of 28.75 cm). Prior to use, the PCB substrate was ultrasonically cleaned in ethanol at 60°C for two minutes. The NiFe and Cu layers were deposited individually, each with its own electrolyte solution. Subsequently, the deposition was repeated to obtain the intended multilayer structure. The NiFe electrolyte solution consisted of 0.099 M $NiSO_4 \cdot 6H_2O$ (Merck), 0.0012 M $FeSO_4 \cdot 7H_2O$ (Merck), 0.149 M H_3BO_3 (Merck), and 1 g/L $C_6H_8O_3$ (Merck), while the Cu electrolyte solution contained 0.065 M $CuSO_4 \cdot 5H_2O$ (Merck), 0.149 M H_3BO_3 (Merck), and 0.0036 M $C_6H_8O_3$ (Merck). The NiFe layer was deposited at a current density of 15.5 mA/cm², and the Cu layer at 8.0 mA/cm². The thickness of each layer was estimated using the deposition rate, namely 1.71 nm/s for the NiFe layer and 2.79 nm/s for the Cu layer. This rate calculation was performed at the beginning of the experiment. To modify the magnetoimpedance ratio, the multilayer samples were fabricated with varying numbers of repetitions (N = 1, 2, 3, and 4) as well as the thickness of the Cu layer (x = 50 nm, 100 nm, 150 nm, and 200 nm).

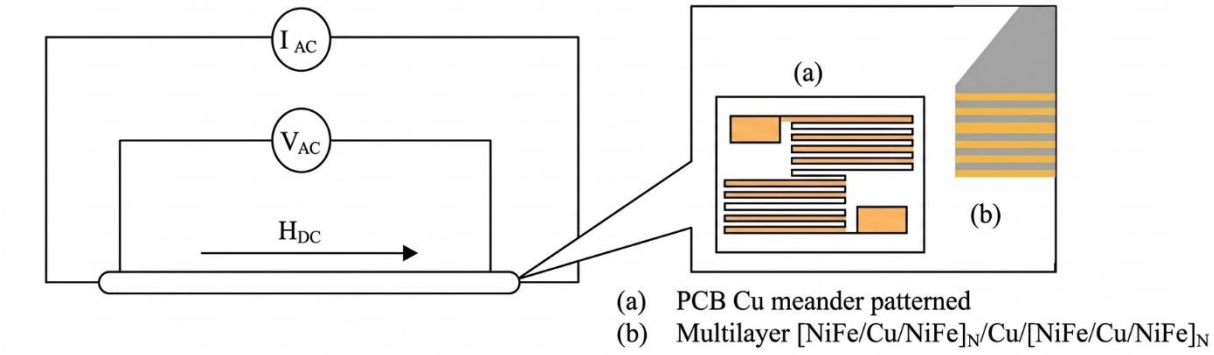


Figure 1. Schematic of the magnetoimpedance measurement setup, showing (a) the Cu PCB meander and (b) the multilayer architecture.

Magnetoimpedance measures the total impedance ($Z = \sqrt{R^2 + X^2}$) of a sample under the influence of an external magnetic field. Where Z is total electrical impedance, R is resistance, and X ($=X_L$-X_C) is the electrical reactance. Measurements were made at a current of 20 mA, at room temperature, and a frequency of 100 kHz. Starting from the initial zero-field condition, the magnetic field with orientation parallel to the film's surface is gradually increased until a maximum of ±80 mT, and the impedance value is measured using an LCR meter (GW Instek GPC 3030 DQ). Once the impedance value becomes nearly constant, the magnetic field is then decreased back to zero, with the total impedance being measured at each field value. Subsequently, the orientation of the magnetic field

is reversed to the negative direction to obtain a complete cycle of the magnetoimpedance curve. The magnetoimpedance ratio is then calculated using Equation (1):

$$\Delta Z/Z(\%) = \frac{Z(H)-Z(H_{max})}{Z(H_{max})} \times 100\% \quad (1)$$

where Z(H) is the measured impedance when a magnetic field H is applied, $Z(H_{max})$ is the measured impedance when the maximum field H_{max} is applied, and H_{max} is the external magnetic field.

Finally, the multilayer sample exhibiting the highest magnetoimpedance (MI) ratio was subsequently assessed for its magnetic sensing performance in detecting cobalt ferrite nanoparticles at quantities of 0.1 g and 0.3 g, respectively. The sensor performance was defined as the change in the MI ratio measured before and after the presence of the nanoparticles. The nanoparticle samples used in this study were self-synthesized La-doped cobalt ferrite, prepared via a co-precipitation method following a previous study (Prasetya et al., 2023).

3. RESULTS AND DISCUSSION

The thickness of both the NiFe and Cu layers increases linearly with deposition time **(**Figure 2**)**. This linear relationship indicates that Faraday's law remains valid for deposition durations of up to 800 seconds for each layer. From the slope of the curves, the deposition rates were determined to be 1.71 nm/s for NiFe and 2.79 nm/s for Cu. By adjusting the deposition time based on these rates, the desired thickness for each NiFe and Cu layer could be fairly achieved, ensuring the reproducibility and reliability of the multilayer samples used in subsequent magnetoimpedance studies and sensor performance evaluations.

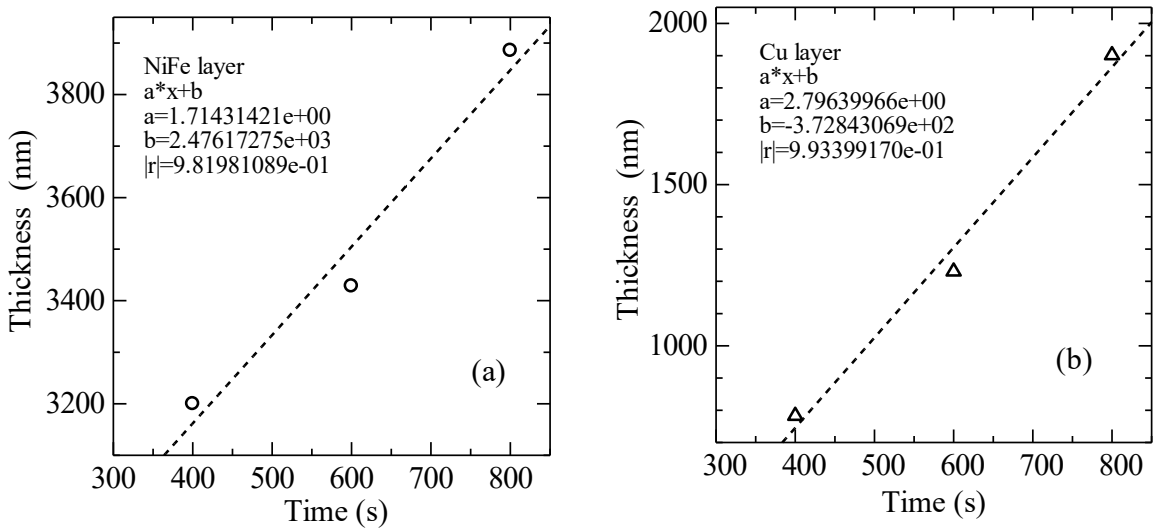


Figure 2. Layer thickness as a function of deposition time for (a) NiFe and (b) Cu. Dashed lines show linear fits.

Figure 3a shows a typical X-ray diffraction (XRD, Bruker D8 Advance, increment 0.02°) pattern of the electrodeposited multilayer sample. The XRD pattern of the Cu substrate is also presented for comparison. It is clearly observed that the deposited thin film exhibits an XRD spectral peak at a diffraction angle (2θ) of 44.44°, which corresponds to the characteristic peak of permalloy (Kharmouche & Cherrad, 2024). This finding confirms that the deposited sample is indeed permalloy. This qualitative analytical result is supported by the X-ray fluorescence (XRF, PANalytical, Type: Minipal 4) analysis presented in Figure 3b, which shows a Ni:Fe compositional ratio of 78.1:21.89. The close agreement between the XRD peak identification and the XRF elemental ratio provides strong evidence for the successful electrodeposition of permalloy layers. The presence of a single, well-defined permalloy peak without additional impurity peaks suggests good crystallinity and phase purity of the deposited films.

Furthermore, the Ni-rich composition, as revealed by XRF, is consistent with the typical permalloy composition (Kharmouche & Taberkani, 2025).

Figure 4(a) shows the magnetic field dependence of the magnetoimpedance (MI) ratio for various numbers of multilayer repetitions (N = 1 – 4), while Figure 4(b) summarizes the corresponding peak MI ratios. As shown in Figure 4(b), the MI ratio increases from 1.02% at N = 1 to 1.65% at N = 2, reaching a maximum value of 2.07% at N = 3. Beyond this optimal condition, the MI ratio declines to 1.78% for N = 4.

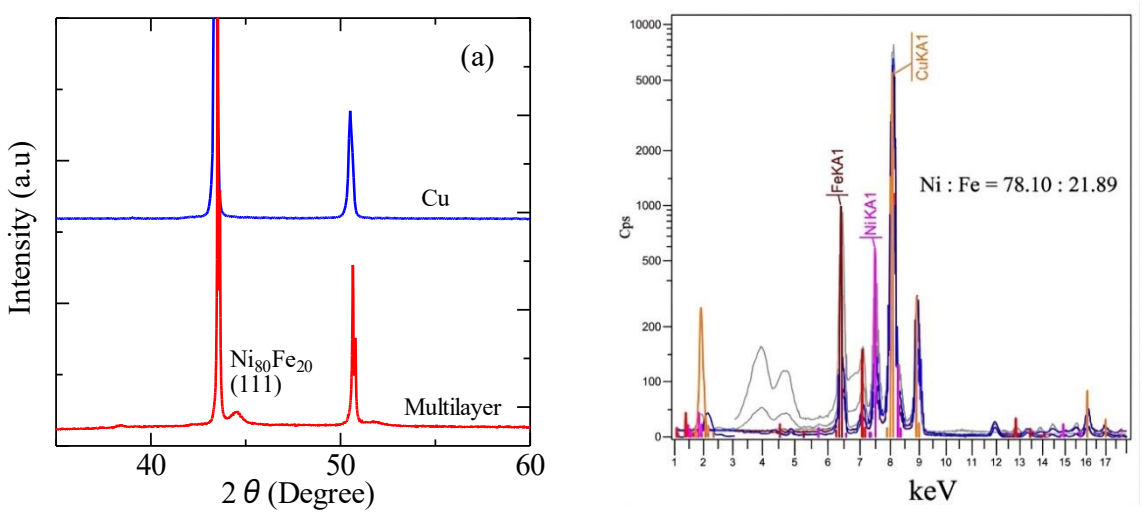


Figure 3. (a) The typical X-ray diffraction (XRD) patterns of Cu substrate and multilayer structure [NiFe(600 nm)/Cu(100 nm)/NiFe(600 nm)]$_3$/Cu (200 nm)/[NiFe(600 nm)/Cu(100 nm)/NiFe(600 nm)]$_3$. (b). X-ray fluorescence (XRF) spectrum of NiFe layer

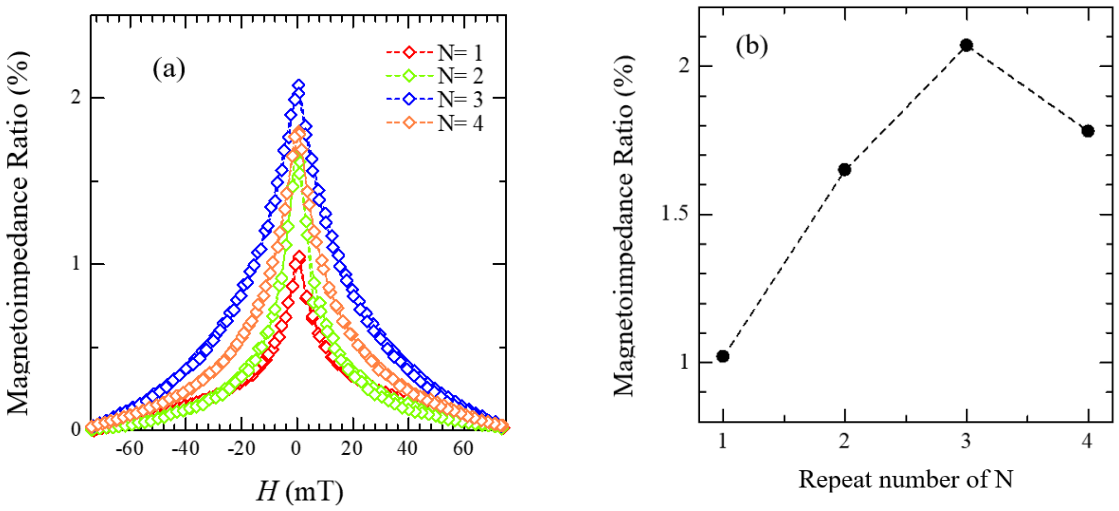


Figure 4 (a) shows the MI ratio versus applied field for different N, (b) shows peak MI ratio versus N of frequency at 100 kHz.

The initial enhancement of the MI ratio with an increasing number of multilayer repetitions (N≤3) is attributed to an improved flux closure effect and higher transverse permeability in the multilayer structure (Phan & Peng, 2008; M. Liu et al., 2023). However, beyond a critical total film thickness (N>3), the MI ratio degrades. This deterioration is likely caused by enhanced eddy current shielding, an increased baseline impedance, and a degradation of soft magnetic properties induced by higher surface roughness and grain growth during prolonged electrodeposition (Kurlyandskaya et al.,

2004). Consequently, these results demonstrate that N= 3 represents the optimal configuration for the tested sample series.

The effect of copper (Cu) layer thickness on the magnetoimpedance (MI) ratio of the $[NiFe(600)/Cu(x)/NiFe(600)]_3/Cu/[NiFe(600)/Cu(x)/NiFe(600)]_3$ multilayer structure was measured at a frequency of 100 kHz as shown in Figure 5(a). The results indicate that variations in Cu layer thickness modify the MI response of these structures.

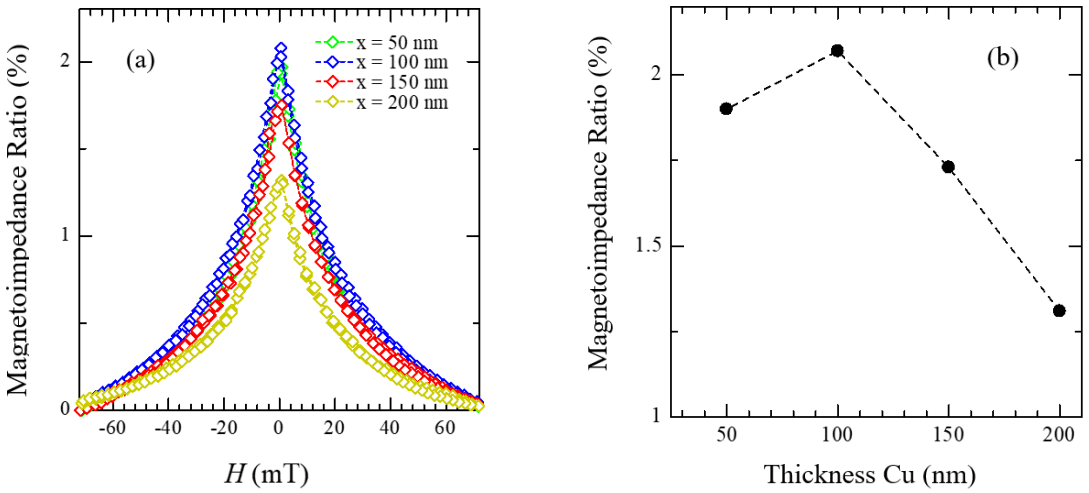


Figure 5 (a). Magnetoimpedance (MI) ratio versus applied magnetic field for different Cu layer thicknesses (x) for the multilayer structure $[NiFe(600\ nm)/Cu(x)/NiFe(600\ nm)]_3/Cu(200\ nm)/[NiFe(600\ nm)/Cu(x)/NiFe(600\ nm)]_3$, where x = 50 nm, 100 nm, 150 nm, and 200 nm. (b) is the peak MI ratio versus x.

As shown in Figure 5b, the MI ratio increases markedly from 1.90% to 2.07% as the Cu layer thickness rises from 50 nm to 100 nm. This observation suggests that the Cu layer thickness plays a crucial role in enhancing the MI response within this multilayer system. The enhancement may be attributed to changes in the magnetic properties and electrical conductivity of the Cu layer with increased thickness, which in turn promote the MI effect (Phan & Peng, 2008). However, it should be noted that when the Cu layer thickness is further increased to 150 nm and 200 nm, the MI ratio decreases to 1.73% and 1.31%, respectively. This trend indicates the existence of an optimal Cu layer thickness that yields the maximum MI ratio, which in this study is observed at 100 nm.

The thickness of the Cu layer also affects the electrical conductivity of the structure. At a thickness of 100 nm, the Cu layer likely provides a more efficient conduction path for electric current, thereby increasing the MI ratio. As a result, changes in the external magnetic field produce greater variations in the electrical resistance of the Cu layer. In addition to conductivity, the Cu layer thickness influences its magnetic properties. The decline in MI response beyond 100 nm suggests that the optimal thickness has been attained. At this point, the Cu layer exhibits the most suitable properties for maximizing the MI effect, and further addition of Cu material leads to a reduction in response. Therefore, optimizing the Cu layer thickness is a critical factor in the development of sensitive MI devices (Yüzüak et al., 2020).

Figure 6 presents the $[NiFe(600\ nm)/Cu(100\ nm)/NiFe(600\ nm)]_3/Cu(200\ nm)/[NiFe(600\ nm)/Cu(100\ nm)/NiFe(600\ nm)]_3$ multilayer magnetoimpedance (MI) sensor for detecting La-doped cobalt ferrite magnetic nanoparticles. The results clearly demonstrate that the MI ratio decreases upon introducing the magnetic nanoparticles to the sensor surface. Specifically, the peak MI ratio drops from an initial value of 2.07% (without nanoparticles) to 1.75% and 1.43% in the presence of 0.1 g and 0.3 g of nanoparticles, respectively. This noticeable reduction in the MI response with increasing nanoparticle mass is attributed to the local stray dipole fields generated by the magnetized cobalt ferrite nanoparticles (Buznikov et al., 2018). When positioned on the surface of the multilayer element, these ferromagnetic particles produce stray magnetic fields that oppose and perturb the external magnetic field. This stray

field induces local magnetic inhomogeneity, disrupts domain wall movement, and pins the transverse magnetization within the soft magnetic NiFe layers. Consequently, the effective transverse permeability of the multilayer structure degrades, which increases the skin depth and dampens the field-induced impedance variation (Panina & Mohri, 2000; Buznikov et al., 2021). The progressive reduction in the peak MI ratio with increasing nanoparticle mass further indicates that the sensor response is dependent on the amount of magnetic material introduced onto its surface. This mass-dependent behavior provides preliminary evidence of the potential applicability of the optimized multilayer structure for quantitative magnetic nanoparticle sensing, although further calibration is required to establish its detection limit and measurement reproducibility. The quantitative decrease in the peak MI ratio confirms that the multilayer system exhibits high sensitivity to varying concentrations of magnetic nanoparticles, making it a suitable candidate for magnetic sensing applications.

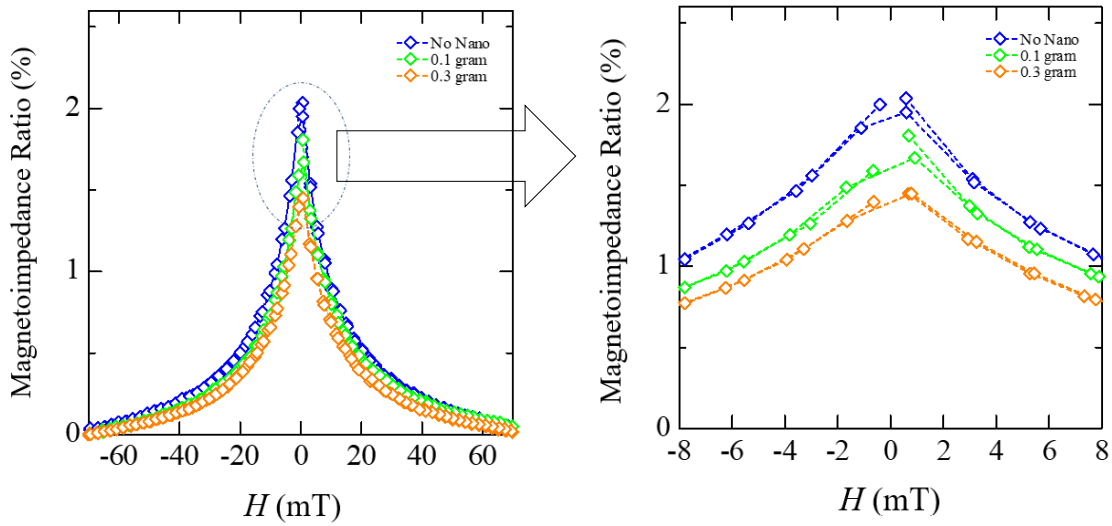


Figure 6. MI ratio versus applied magnetic field for the selected multilayer without nanoparticles and with the verified cobalt ferrite masses; the right panel expands the low-field region.

4. CONCLUSION

The magnetoimpedance effect has been successfully observed in a multilayer system of [NiFe(600 nm)/Cu(x)/NiFe(600 nm)]N/Cu (200 nm)/[NiFe(600 nm)/Cu(x)/NiFe(600 nm)]$_N$ permalloy multilayer structures deposited on Cu PCB meander-patterned substrates via the electrodeposition method. This study evaluates the effects of repetition number (N) and Cu spacer thickness (x) on the magnetoimpedance (MI) ratio. At 100 kHz, the highest MI ratio of 2.07% is achieved for N=3 and x=100 nm, attributed to an optimal balance between magnetic permeability and electrical conductivity. Furthermore, the multilayer sensor effectively detects cobalt ferrite nanoparticles, with MI discrepancies of 0.32 and 0.64 for 0.1 g and 0.3 g masses, respectively. These findings demonstrate a mass-dependent MI response and highlight the importance of multilayer structural optimization in developing magnetic sensing elements. The integration of electrodeposited NiFe/Cu multilayers with meander-patterned substrates therefore provides a promising approach for low-frequency magnetic nanoparticle detection. Further investigations focusing on sensor calibration, reproducibility, and detection limits are recommended to establish its potential for quantitative sensing applications.

AUTHOR CONTRIBUTIONS

Conceptualization, B.P.; methodology, A.D.S.; formal analysis, N.P.P. and I.; data curation, F.W. and P.K.; writing—original draft preparation, A.D.S.; writing—review and editing, N.P.P. and B.P.; supervision, B.P.; project administration, R.; funding acquisition, R.

FUNDING

This research was funded by Universitas Sebelas Maret through the 2026 RKAT Penguatan Kapasitas Grup Riset (PKGR-UNS) scheme, contract number 462/UN27.22/PT.01.03/2026.

DATA AVAILABILITY STATEMENT

The data supporting the findings of this study are available from the corresponding author upon reasonable request.

CONFLICTS OF INTEREST

The authors declare no conflict of interest.

ARTIFICIAL INTELLIGENCE (AI) USAGE DECLARATION

The authors acknowledge the use of generative AI tools (Grammarly) in the preparation of this manuscript, specifically for language editing and grammar correction. No content generation or data interpretation was performed by AI. The authors take full responsibility for the content and conclusions of this work.

REFERENCES

Barrera, G., Celegato, F., Vassallo, M., Martella, D., Coïsson, M., Olivetti, E. S., Martino, L., Sözeri, H., Manzin, A., & Tiberto, P. (2024). Microfluidic detection of SPIONs and Co-ferrite ferrofluid using amorphous wire magneto-impedance sensor. *Sensors, 24*(15), 4902. https://doi.org/10.3390/s24154902

Beach, R. S., & Berkowitz, A. E. (1994). Giant magnetic field dependent impedance of amorphous FeCoSiB wire. *Applied Physics Letters, 64*(26), 3652–3654. https://doi.org/10.1063/1.111170

Beato-López, J. J., Algueta-Miguel, J. M., & Gómez-Polo, C. (2021). Contactless magnetic nanoparticle detection platform based on non-linear GMI effect. *Measurement, 180*, 109602. https://doi.org/10.1016/j.measurement.2021.109602

Beato-López, J. J., Pérez-Landazábal, J. I., & Gómez-Polo, C. (2018). Enhanced magnetic nanoparticle detection sensitivity in non-linear magnetoimpedance-based sensor. *IEEE Sensors Journal, 18*(21), 8701–8708. https://doi.org/10.1109/JSEN.2018.2868860

Buznikov, N. A., & Kurlyandskaya, G. V. (2019). Magnetoimpedance in symmetric and non-symmetric nanostructured multilayers: A theoretical study. *Sensors, 19*(8), 1761. https://doi.org/10.3390/s19081761

Buznikov, N. A., Safronov, A. P., Orue, I., Golubeva, E. V., Lepalovskij, V. N., Svalov, A. V., Chlenova, A. A., & Kurlyandskaya, G. V. (2018). Modelling of magnetoimpedance response of thin film sensitive element in the presence of ferrogel: Next step toward development of biosensor for in-tissue embedded magnetic nanoparticles detection. *Biosensors and Bioelectronics, 117*, 366–372. https://doi.org/10.1016/j.bios.2018.06.032

Buznikov, N. A., Svalov, A. V., & Kurlyandskaya, G. V. (2021). Influence of the parameters of permalloy-based multilayer film structures on the sensitivity of magnetic impedance effect. *Physics of Metals and Metallography, 122*(3), 223–229. https://doi.org/10.1134/S0031918X21030029

Chlenova, A. A., Moiseev, A. A., Derevyanko, M. S., Semirov, A. V., Lepalovsky, V. N., & Kurlyandskaya, G. V. (2017). Permalloy-based thin film structures: Magnetic properties and the giant magnetoimpedance effect in the temperature range important for biomedical applications. *Sensors, 17*(8), 1900. https://doi.org/10.3390/s17081900

de Melo, A. S., Bohn, F., Ferreira, A., Vaz, F., & Correa, M. A. (2020). High-frequency magnetoimpedance effect in meander-line trilayered films. *Journal of Magnetism and Magnetic Materials, 515*, 167166. https://doi.org/10.1016/j.jmmm.2020.167166

García-Arribas, A., Fernández, E., Svalov, A., Kurlyandskaya, G. V., & Barandiaran, J. M. (2016). Thin-film magneto-impedance structures with very large sensitivity. *Journal of Magnetism and Magnetic Materials, 400*, 321–326. https://doi.org/10.1016/j.jmmm.2015.07.107

Jimenez, V. O., Hwang, K. Y., Nguyen, D., Rahman, Y., Albrecht, C., Senator, B., Thiabgoh, O., Devkota, J., Bui, V. D. A., Lam, D. S., Eggers, T., & Phan, M.-H. (2022). Magnetoimpedance biosensors and real-time healthcare monitors: Progress, opportunities, and challenges. *Biosensors, 12*(7), 517. https://doi.org/10.3390/bios12070517

Kharmouche, A., & Cherrad, O. (2024). Structural, microstructural and morphological properties of Permalloy/Si(100) thin films. *Physica B: Condensed Matter, 680*, 415803. https://doi.org/10.1016/j.physb.2024.415803

Kharmouche, A., & Taberkani, L. (2025). Thickness-dependent electrical and magnetic properties of Permalloy thin films. *Journal of Materials Science: Materials in Electronics, 36*(16), 959. https://doi.org/10.1007/s10854-025-15018-0

Kikuchi, H., Tanii, M., & Umezaki, T. (2020). Effects of parallel and meander configuration on thin-film magnetoimpedance element. *AIP Advances, 10*(1), 015334. https://doi.org/10.1063/1.5130410

Kilic, U., Ross, C. A., & Garcia, C. (2018). Tailoring the asymmetric magnetoimpedance response in exchange-biased Ni-Fe multilayers. *Physical Review Applied, 10*(3), 034043. https://doi.org/10.1103/PhysRevApplied.10.034043

Kurlyandskaya, G. V., Elbaile, L., Alves, F., Ahamada, B., Barrué, R., Svalov, A. V., & Vas'kovskiy, V. O. (2004). Domain structure and magnetization process of a giant magnetoimpedance geometry FeNi/Cu/FeNi(Cu)FeNi/Cu/FeNi sensitive element. *Journal of Physics: Condensed Matter, 16*(36), 6561–6568. https://doi.org/10.1088/0953-8984/16/36/021

Licarião, R. J. C., de Lima, J. D. M., França, E. L. T., Rodrigues, A. R., Padrón-Hernández, E., Machado, F. L. A., & Vilela, G. L. S. (2025). Giant magneto-impedance effect in CoP/Cu bilayers meander-like sensing elements. *Journal of Applied Physics, 138*(3), 034505. https://doi.org/10.1063/5.0271750

Liu, M., Wang, Z., Meng, Z., Sun, X., Huang, Y., Guo, Y., & Yang, Z. (2023). Giant magnetoimpedance effect of multilayered thin film meanders formed on flexible substrates. *Micromachines, 14*(5), 1002. https://doi.org/10.3390/mi14051002

Melnikov, G. Y., Komogortsev, S. V., Svalov, A. V., Gorchakovskiy, A. A., Vazhenina, I. G., & Kurlyandskaya, G. V. (2024). Effects of magnetostatic interactions in FeNi-based multilayered magnetoimpedance elements. *Sensors, 24*(19), 6308. https://doi.org/10.3390/s24196308

Melnikov, G. Y., Lepalovskij, V. N., Svalov, A. V., Safronov, A. P., & Kurlyandskaya, G. V. (2021). Magnetoimpedance thin film sensor for detecting of stray fields of magnetic particles in blood vessel. *Sensors, 21*(11), 3621. https://doi.org/10.3390/s21113621

Oktaria, V., Putra, C. T., Sutomo, A. D., Utari, & Purnama, B. (2020). Effect of multilayer structure parameters on magneto-impedance ratio with low frequency measurements. *Journal of Physics: Theories and Applications, 4*(1), 29–35. https://doi.org/10.20961/jphystheor-appl.v4i1.44694

Panina, L. V., & Mohri, K. (1994). Magneto-impedance effect in amorphous wires. *Applied Physics Letters, 65*(9), 1189–1191. https://doi.org/10.1063/1.112104

Panina, L. V., & Mohri, K. (2000). Magneto-impedance in multilayer films. *Sensors and Actuators A: Physical, 81*(1–3), 71–77. https://doi.org/10.1016/S0924-4247(99)00089-8

Phan, M.-H., & Peng, H.-X. (2008). Giant magnetoimpedance materials: Fundamentals and applications. *Progress in Materials Science, 53*(2), 323–420. https://doi.org/10.1016/j.pmatsci.2007.05.003

Prasetya, N. P., Setiyani, R. I., Utari, Kusumandari, K., Iriani, Y., Safani, J., Taufiq, A., Wibowo, N. A., Suharno, S., & Purnama, B. (2023). Cation trivalent tune of crystalline structure and magnetic properties in coprecipitated cobalt ferrite nanoparticles. *Materials Research Express, 10*(3), 036102. https://doi.org/10.1088/2053-1591/acc011

Rusydan, D. A., Ismail, Sutomo, A. D., Utari, & Purnama, B. (2021). The influence of AC driving current on magnetoimpedance in [Ni80Fe20/Cu]x/Cu/[Ni80Fe20/Cu]6−x multilayers. *Journal of Physics: Theories and Applications, 5*(1), 44–50. https://doi.org/10.20961/jphystheor-appl.v5i1.52259

Rusydan, D. A., Purnama, B., Utari, & Sutomo, A. D. (2022). Effect of annealing temperature to magnetoimpedance on multilayer film [Ni80Fe20/Cu]x/Cu/[Ni80Fe20/Cu]6-x for symmetry and non-symmetry structures. *AIP Conference Proceedings, 2391*(1), 070003. https://doi.org/10.1063/5.0072431

Sayad, A., Uddin, S. M., Chan, J., Skafidas, E., & Kwan, P. (2021). Meander thin-film biosensor fabrication to investigate the influence of structural parameters on the magneto-impedance effect. *Sensors, 21*(19), 6514. https://doi.org/10.3390/s21196514

Sutomo, A. D., Kusumawardhani, P., Yasmin, H. H., Handayani, R., Yusri, Ismail, Utari, Ramelan, A. H., Nuryani, & Purnama, B. (2023). Saccharin dependence of magnetoimpedance ratio in electrodeposited permalloy

multilayer structure on meandered-copper printed-circuit-board substrates. *Trends in Sciences, 20*(11), 6695. https://doi.org/10.48048/tis.2023.6695

Tandon, P., Sahu, R., Mishra, A. C., Singh, K., Srikanti, K., & Gopalan, R. (2023). Magnetoimpedance effect in electrodeposited NiFe/Cu wire using trisodium citrate additive in plating bath. *Journal of Magnetism and Magnetic Materials, 570*, 170490. https://doi.org/10.1016/j.jmmm.2023.170490

Vasam, S., & Veeturi, S. (2022). Magnetoimpedance in electrodeposited NiFe/Cu composite wires: A study on role of in-situ stress. *Solid State Communications, 343*, 114643. https://doi.org/10.1016/j.ssc.2021.114643

Yüzüak, G. D., Yüzüak, E., & Nevruzoğlu, V. (2020). Magneto-impedance in Co35Fe65/Cu/Co35Fe65 single and bi-layer thin films. *Electronic Materials Letters, 16*(5), 473–480. https://doi.org/10.1007/s13391-020-00237-w